

## INTERACTION OF A GIANT PLANET IN AN INCLINED ORBIT WITH A CIRCUMSTELLAR DISK

F. MARZARI<sup>1</sup> AND ANDREW F. NELSON<sup>2</sup>

<sup>1</sup> Università di Padova, Dipartimento di Fisica, via Marzolo 8, 35131 Padova, Italy; francesco.marzari@pd.infn.it

<sup>2</sup> HPC-5, Los Alamos National Laboratory, Los Alamos, NM 87544, USA; andy.nelson@lanl.gov

Received 2009 June 16; accepted 2009 September 28; published 2009 October 23

### ABSTRACT

We investigate the dynamical evolution of a Jovian-mass planet injected into an orbit highly inclined with respect to its nesting gaseous disk. Planet–planet scattering induced by convergent planetary migration and mean motion resonances may push a planet into such an out-of-plane configuration with inclinations as large as  $20^\circ$ – $30^\circ$ . In this scenario, the tidal interaction of the planet with the disk is more complex and, in addition to the usual Lindblad and corotation resonances, it also involves inclination resonances responsible for bending waves. We have performed three-dimensional hydrodynamic simulations of the disk and of its interactions with the planet with a smoothed particle hydrodynamics code. A main result is that the initial large eccentricity and inclination of the planetary orbit are rapidly damped on a timescale of the order of  $10^3$  yr, almost independently of the initial semimajor axis and eccentricity of the planet. The disk is warped in response to the planet perturbations and it precesses. Inward migration also occurs when the planet is inclined, and it has a drift rate that is intermediate between type I and type II migration. The planet is not able to open a gap until its inclination becomes lower than  $\sim 10^\circ$ , when it also begins to accrete a significant amount of mass from the disk.

*Key words:* planetary systems – planetary systems: formation

*Online-only material:* color figures

### 1. INTRODUCTION

Planet migration has been recognized as a key mechanism of evolution for planetary systems. Torques on a planet, arising from interactions with the circumstellar disk, can cause a planet to move a considerable distance from the orbit where it formed into a new dynamical configuration, possibly explaining the many observed giant planets moving on trajectories well within the ice condensation line and very close to the parent star. Unfortunately, it cannot explain the highly elliptical orbits of many of the extrasolar planets discovered to date. The most likely explanation for these objects is that another mechanism comes into play in the early phases of evolution of a planetary system: planet–planet scattering. When two or more planets form from the protoplanetary disk, they may come very near to each other and begin a period of chaotic evolution dominated by mutual close encounters. In such a scenario, one (or more) of the planets can be ejected from the system entirely, leaving the remaining planets with eccentric orbits. This mechanism, in its classical formulation (Weidenschilling & Marzari 1996; Marzari & Weidenschilling 2002; Rasio & Ford 1996; Chatterjee et al. 2008), is based on the assumption that the planets emerge from the protoplanetary disk, after the dissipation of the gaseous component, on orbits which are packed together closely enough to be unstable. The subsequent evolution in a gas-free scenario dramatically alters the initial orbital structure of the multi-planet system, ejecting bodies out of the system and causing the growth of the eccentricity and mutual inclination of the surviving planets in the system.

Orbital migration by tidal interaction with the disk and by planet–planet scattering are usually studied as separate mechanisms occurring at different evolutionary stages of a planetary system. However, it is likely that they acted together if the protostellar disk does not dissipate shortly after the formation of Jovian planets. Recent numerical models by Alibert et al. (2005) show that giant planet formation may require only  $10^5$ – $10^6$  yr to

occur, although many uncertainties remain in understanding the process. As a consequence, a multi-planet system may already be formed while the bodies are still embedded within the disk. The subsequent type I or type II migration (Ward 1997) may lead any pair of planets to come closer than their stability limit and start a planet–planet scattering phase. The chaotic evolution dominates the subsequent evolution of the planets and the outcome is not significantly different from the gas-free scenario. At the end of the scattering phase, if the gas component of the disk is still present, the tidal interaction between the disk and the surviving planets may still modify the final configuration of the system by moving the planets close to the star or by circularizing their orbits.

Planet migration after a planet–planet scattering phase has to account for the high eccentric and inclined orbits the planets have acquired during the chaotic evolution. So far, both analytical and numerical works have studied migration of giant planets mainly in the context of initially circular orbits coplanar to the protoplanetary disk. Moorhead & Adams (2005) considered two-planets systems evolving under the action of disk torques (type II migration) and planet–planet scattering. If the planets formed sufficiently close together or moved closer to each other during their formation process while they evolved under the action of type I migration, which depends on the mass of the body, their combined tidal effects would cause the region between them to be cleared because of overlapping Lindblad resonances. Hydrodynamic simulations (Snellgrove et al. 2001; Papaloizou 2003; Kley et al. 2004, 2005; Nelson & Benz 2003a, 2003b) show that the timescale for clearing is only a few hundred orbital periods and also that, in many cases, the region inside the inner planet orbit quickly loses material due to accretion onto the host star. The inner planet does not migrate because there is no disk material left close to it to generate torques. On the other hand, the outer disk exerts negative torques at the Lindblad resonances of the outer planet possibly causing it to migrate inward moving closer to the inner one.

Convergent orbital migration due to different drift rates may cause planets to end up either in resonance or to move into crossing trajectories that eventually start a chaotic scattering phase, in turn frequently causing a planet to be ejected. The surviving planet is left on an eccentric and inclined orbit that is evolved, in the model of Moorhead & Adams (2005), with the usual migration rate of a planar orbit. However, if the planet orbit is out of the disk plane, its inward orbital migration may be significantly different from the planar case. The interaction between the planet's gravitational field and the gas is complicated by the dynamical effects related to the inclination between the disk and the planet. The planet might be unable to clean and maintain a gap in the disk, but still generate waves at Lindblad and vertical resonances and cause torques that dominate the dynamical evolution of the planet. The high eccentricity that a planet typically acquires after the chaotic phase might also reverse the migration trend away from the star, as shown by Papaloizou & Larwood (2000). Disk warping in response to the secular perturbations of the planet might lead, through dissipation, to damping of the inclination (Lubow & Ogilvie 2001), though we note that his conclusions are derived under the assumption that the planet opens a gap in the disk, splitting it in two rings. These are all aspects that need a detailed investigation from a numerical point of view.

An additional mechanism that can excite the inclination of a giant planet embedded in a disk is captured in mean motion resonance. Thommes & Lissauer (2003) have shown that two Jupiter-mass planets on converging orbits may enter inclination resonances during their evolution. These resonances induce rapid growth of the inclinations of both planets which end up in highly non-coplanar configurations. According to their simulations, once the planets are trapped in a 2:1 mean motion resonance, their eccentricities are excited while they migrate together toward the star. During this evolution the planets may enter a 4:2 second-order inclination-type resonance whose critical arguments include the node longitudes. The inclinations of both bodies increase rapidly and the inner planet may achieve an inclination larger than  $\sim 20^\circ$  in some tens of thousands of years, while the eccentricity of both bodies keep growing. After a while, the system moves out of resonance with a further abrupt increase in inclinations. The important condition for this resonance to occur is that the mass ratio between the inner planet and the outer planet is not smaller than two. Otherwise, the innermost massive body cannot gain enough eccentricity to enter the inclination-type resonance. Another critical aspect of the resonant evolution is the amount of eccentricity damping by the disk. If it is too strong, it might prevent the planets from reaching the critical eccentricity that opens the door for inclination-type resonances.

In this paper, we concentrate on the orbital evolution of a giant planet injected into a highly inclined, highly eccentric orbit respect to the disk. This may have occurred either after a planet-planet scattering phase or once captured in an inclination-type resonance and escaped from it. In both cases, we expect not only a high inclination but also a large eccentricity. We will investigate the kind of orbital migration the planet undergoes and the timescale of its eccentricity and inclination damping. Previous studies (Tanaka & Ward 2004; Papaloizou & Larwood 2000) focused on the three-dimensional interaction between small planets and the disk with eccentricities and inclinations smaller than the disk aspect ratio. In this regime, the effects of density and bending waves on the planet evolution have been analytically computed with a linear model, with Tanaka &

Ward (2004) predicting damping times for both eccentricity and inclination of the order of  $300(r/1 \text{ AU})^2$ . Cresswell et al. (2007) numerically simulated the evolution of small mass planets (up to 20 Earth-mass) on orbits with eccentricities up to  $e = 0.3$  and a maximum inclination relative to the disk of  $10^\circ$  via three-dimensional hydrodynamic simulations, beyond the range of validity of the Tanaka & Ward (2004) analytical model. From their fit to the data in a high eccentricity ( $e = 0.3$ ) and high-inclination regime ( $i = 8^\circ$ ), the damping time of both  $e$  and  $i$  to low values is approximately of the order of 400 orbital periods ( $\sim 4700 \text{ yr}$ ) for a planet at 5.2 AU. Also, they always find inward migration, even if reduced for large  $e$  and  $i$ .

Here, we consider three-dimensional simulations of massive planets (one Jupiter mass) evolving on highly inclined ( $20^\circ$ ) and eccentric ( $e = 0.4$ ) orbits. The scenarios are different since the evolutionary history leading to the high-inclination orbit is distinct. Moreover, the migration mechanism is expected to be significantly different due to the large mass we consider compared to that analyzed in previous models. The linear regime adopted by Tanaka & Ward (2004) to model density and bending waves does not hold in the case we consider and, in addition, the disk is also significantly warped in response to the planet perturbations.

In Section 2, we describe the initial conditions and numerical techniques; while in Section 3, we describe the results of the simulations. In Section 4, we comment our results and discuss future work.

## 2. INITIAL CONDITIONS AND PHYSICAL MODEL

The systems we simulate consist of three components: a star, a planet, and a disk. We model these systems using the publically available code, VINE, (Wetzstein et al. 2009; Nelson et al. 2009) to model the combined system in three spatial dimensions, using the particle-based “smoothed particle hydrodynamics” (SPH) method. This code has previously been used by one of us in extensive simulations of circumstellar disks (e.g., Nelson et al. 2000; Nelson 2006) and is known to perform well in such configurations.

We define the star and planet to have mass  $1 M_\odot$  and  $1 M_J$ , respectively, and to be in Keplerian orbits around their common center of mass. The orbit is eccentric, with  $e$  ranging from 0.0 to 0.4 in different simulations, and inclined respect to the disk plane (defined below) by  $i = 20^\circ$ . We consider three different initial semimajor axes for the planet: 2, 4, and 6 AU. These orbital parameters can easily be achieved either after a phase of planet-planet scattering or because of resonant pumping as described in Thommes & Lissauer (2003). The star and the disk are each modeled as Plummer softened point masses, with softening lengths of 0.25 AU and 0.05 AU, respectively. Self-gravity for the disk, when included in our simulations, is calculated using an approximate, tree-based summation of particles and aggregates of particles, with parameters set such that the maximum force errors are smaller than  $\sim 0.1\%$ .

We define the initial condition of the disk as follows. At time zero, we set approximately 450,000 equal mass particles on a series of concentric rings extending from an innermost ring at a distance of 0.5 AU from the star, to an outer radius at 13 AU. Disk matter is set up on initially circular orbits assuming a Keplerian rotation curve. Radial velocities are set to zero. The distribution of disk material is defined by a surface density power

law of the form

$$\Sigma(r) = S\Sigma_0 \left[ 1 + \left( \frac{r}{r_c} \right)^2 \right]^{-\frac{p}{2}}, \quad (1)$$

where  $\Sigma_0 = 15,500 \text{ gm cm}^{-2}$ ,  $p = 3/2$ , and  $r_c = 0.25 \text{ AU}$ . These parameters yield a disk mass of approximately  $0.0078 M_\odot$ , or just over  $8 M_J$ . In order to avoid numerical instabilities in the initial condition associated with a too sharp outer disk edge, we include a softening function,  $S$ , in the specification of the surface density, as originally specified in Nelson (2006). This function extends  $\pm\delta = 1 \text{ AU}$  in each direction from the nominal outer disk edge, and alters the surface density using a function which decreases linearly to zero over the range, so that the disk's final dimensions extend to  $14 \text{ AU}$ . The distribution of particles in the vertical coordinate is specified below.

The temperature profile is specified by a similar power law of the form:

$$T(r) = T_0 \left[ 1 + \left( \frac{r}{r_c} \right)^2 \right]^{-\frac{q}{2}}, \quad (2)$$

where  $T_0 = 340 \text{ K}$ ,  $q = 1/2$ , and  $r_c$  is as above. With these parameters, the ‘‘snow line,’’ at which planet formation is expected to be enhanced, falls at  $r \approx 3.9 \text{ AU}$ . We employ a locally isothermal equation of state to close the system of hydrodynamic equations, with temperature at any given radius always specified exactly by Equation (2) and the pressure specified by the relation  $p = \rho c_s^2$ , where  $c_s$  is the sound speed. This choice permits a computationally simple description of the disk thermodynamics at the cost of restricting the physical interpretation given to the simulations. In some circumstances, for example, it may permit gas to compress to much greater densities than would otherwise be the case. We refer the reader to Durisen et al. (2007) for a more complete discussion. These restrictions will incur no great burden on our calculations except in the neighborhood of the planet, where they may become inaccurate, particularly when appreciable disk material collects there as it does at late times in our simulations. We must therefore be cautious in our interpretations of the behavior at such times.

The choice of an isothermal equation of state constrains the vertical density structure of the disk to be a Gaussian function of the  $z$ -coordinate, with a scale height,  $H = c_s/\Omega$  (see, e.g., Nelson 2006). The specification of the initial condition will be complete once we incorporate this constraint. We do so by assigning a value to the  $z$ -coordinate for each particle using the locally defined isothermal scale height, multiplied by pseudorandom number drawn from a Gaussian distribution.

With the initial conditions described above, the value of the well-known Toomre stability parameter is well above  $Q = 20$  everywhere in the disk. Therefore, we expect the system to be stable to self-gravitating disturbances. Nevertheless, self-gravity may remain an important effect because of its influence on the radial positions of resonances in the disk (Nelson & Benz 2003b), which in turn affect the strength of gravitational torques on the planet and its migration.

As a final check on our initial condition, we have verified that our simulations obey minimum resolution requirements, below which the numerical methods fail to reproduce known behavior of the system accurately. Following the procedure described in Nelson (2006), we have generated a replica of our initial condition without a planet, and evolved it for  $300 \text{ yr}$  in order to permit a stable numerical equilibrium condition to

evolve for the vertical structure. We then performed empirical fits to the vertical disk structure as realized in this simulation, and compared the parameters obtained from these fits to their analytically expected values. This exercise demonstrates that our simulations are adequately resolved, with ratios of fit to analytic midplane densities above 90% over the radius ranges of interest to our calculations.

### 3. RESULTS

Using the initial conditions and the physical model described above, we have run a family of similar simulations of the evolution of a planet initially in an orbit inclined to a circumstellar disk. In the following sections, we first describe the evolution of a prototype model, and then a number of variations upon it. Our prototype model is of a planet initially orbiting its parent star with a semimajor axis of  $4 \text{ AU}$ , eccentricity  $e = 0.4$ , and with its orbital plane inclined by  $i = 20^\circ$  to a circumstellar disk, for which we neglect the self-gravitating effects of the disk on itself. The first variation consists in including disk self-gravity and exploring how it affects the planet evolution. We then change the numerical resolution considering a model with a higher and one with a lower number of SPH particles. Two simulations are devoted to study the changes in evolution when the planet's semimajor axis is either  $2$  or  $6 \text{ AU}$ , and two when the planet's initial eccentricity is reduced to  $e = 0$  and  $e = 0.2$ . Finally, we study the evolution of the planet's motion when the disk has an internal cavity, into which a planet is assumed to have been scattered on to an orbit with semimajor axis of  $2 \text{ AU}$ .

#### 3.1. Evolution of Systems with and without Disk Self-gravity

Self-gravity may play an important role in the evolution of a planet interacting with the disk. A number of previous works (Nelson & Benz 2003a, 2003b; Baruteau & Masset 2008) have shown that the inclusion of disk self-gravity in numerical hydrodynamic models lead to a different value of the differential Lindblad torque and may indeed affect the computed migration rate of a planet embedded in the disk. For this reason, we performed two simulations with the same initial parameters for both the planet and the disk; but in one case we took into account disk self-gravity.

##### 3.1.1. Orbital Evolution of the Planet

In Figure 1, we show that the evolution of the planet orbital elements with the planet started on an orbit with semimajor axis  $a = 4 \text{ AU}$ , eccentricity  $0.4$ , and inclination  $20^\circ$ . The exchange of angular momentum between the disk and the planet causes all of the planet's orbital elements to evolve significantly over the  $\sim 1000 \text{ yr}$  timescale we simulate here, in both simulations. Overall, both simulations show essentially identical behavior, and we conclude that disk self-gravity is not an important effect in systems like those in our study. Therefore, in the interests of numerical simplicity, we will neglect it in our remaining discussions.

As the systems evolve, the planet undergoes inward orbital migration at a rate of  $\sim 1.5 \text{ AU per } 10^4 \text{ yr}$ , consistent with analytic theories of type I migration (Tanaka et al. 2002), but for planet of terrestrial mass. Due to the large initial inclination of the planet, it is expected that not only Lindblad and corotation resonances cause the disk-planet coupling but also vertical resonances (Murray & Dermott 1999; Griv 2007; Tanaka & Ward 2004) play a significant role. These resonances have the node longitude of the planet and that of the ring at the resonant

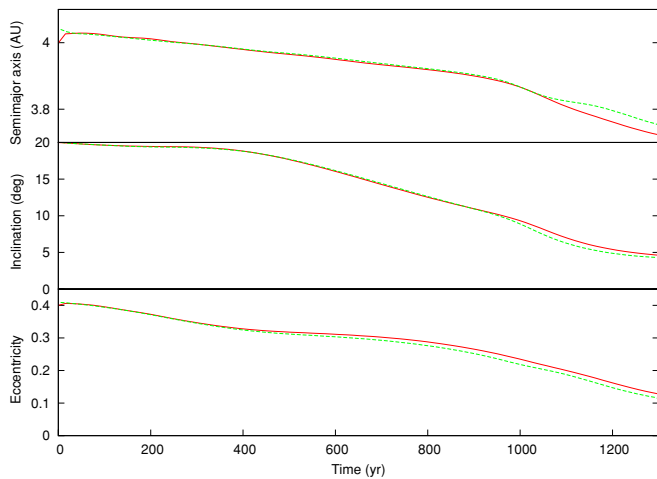


**Figure 1.** Evolution of the orbital elements of planets residing in disks with (continuous line) and without (dashed line) self-gravity. From top to bottom, we show semimajor axis, eccentricity, and inclination as functions of time.

(A color version of this figure is available in the online journal.)

location within their resonant argument. It is well known that the existence of vertical resonances with Mimas give rise to bending waves in the Saturn rings. The combination of eccentric and bending waves, in particular, in the initial phase of the planet evolution when it is well out of plane, makes it difficult to predict analytically all the torques acting on the planet. In addition, and as we will show below, the disk becomes warped and precesses, adding further complexity to the problem. Our scenario is significantly different from that described by Tanaka & Ward (2004) since we consider a Jovian-type planet and values of eccentricity and inclination by far larger than the disk aspect ratio. Therefore, we limit ourselves to give the numerical value of the migration rate.

Most significantly in the context of our interest in the outcomes of planet–planet scattering, both the planet’s eccentricity and its inclination are quickly damped by its interaction with the disk. Although the interaction strength between disk and planet are clearly highly time dependent at early times as the planet successively dives through the disk midplane and climbs out of it during its orbit, both inclination and eccentricity decay at near constant rates until relatively late in the simulations. The decay accelerates significantly after  $\sim 800$ – $1000$  yr of evolution, as the planet spends more and more time close to the midplane where densities are high. At approximately the same time, they begin to accumulate an envelope of disk material because of their longer duration passages through the midplane. We will discuss the numerical and physical significance of the envelope mass accumulation in Section 3.5.

### 3.1.2. Evolution of the Disk Morphology

Figure 2(a) shows the disk surface density morphology for the simulation with self-gravity, projected onto the  $(x, y)$  plane after 500 yr. Spiral structures generated by the tidal interactions between planet and disk extend inward and outward from its position, demonstrating the effect of Lindblad resonances on the evolution. No low-density gap has yet developed at this time, nor does one develop later, until the planet’s trajectory decays to an orbit where it again spends most of its time embedded in high-density disk material.

The out-of-plane perturbations of the planet leads to a warped structure of the disk, as shown in the projection plot

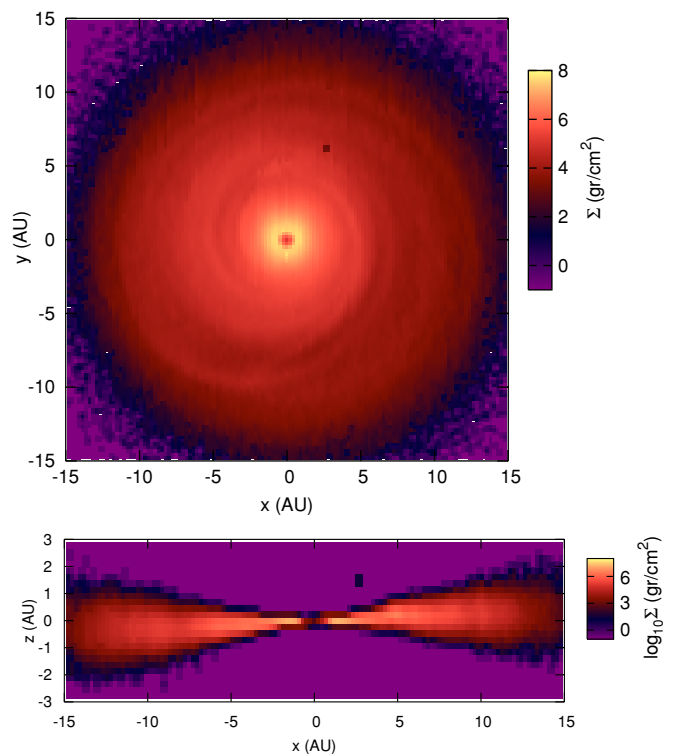


**Figure 2.** Density distribution of the disk after 500 yr from the beginning of the simulation where the disk is unperturbed. In the top plot, we show the logarithm of the disk density ( $\text{g cm}^{-2}$ ) on the  $(x, y)$  plane while an angular section of the disk projected in the  $(z, y)$  plane is shown in the bottom plot. The position of the planet is marked by a black square in both plots.

(A color version of this figure is available in the online journal.)

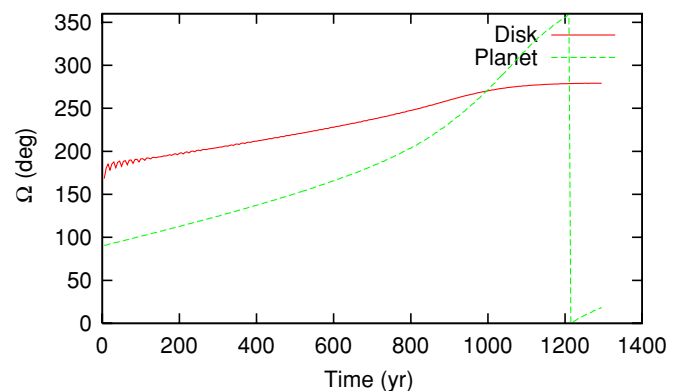


**Figure 3.** Evolution of the node longitude of the disk (continuous line) and planet (dashed line). The precession of the disk is slower as the planet dives into the disk on low-inclination orbits.

(A color version of this figure is available in the online journal.)

of Figure 2(b), and to its precession. The shape of the disk in the  $(x, z)$  plane is similar to that found by Larwood et al. (1996), who modeled the evolution of a disk in a binary system not coplanar to the companion orbit. Our scenario is similar to theirs, with the planet being less massive than a binary companion but closer to the star and the disk. In Figure 3, we show the evolution of the node longitude of both the planet and the disk, respect to the starting reference frame, when the planet has an initial semimajor axis of 6 AU. The precession of the disk is fast when the planet is far from the disk plane and it slowly decreases when the orbit of the planet becomes less inclined.

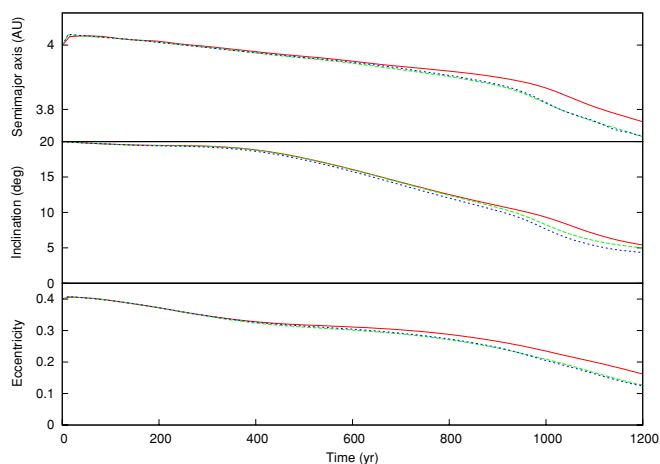


**Figure 4.** Evolution of the orbital elements of planets residing in disks resolved at low (blue dashed line), standard (red continuous line), and high (green dashed line) numerical resolution, as defined in the text. Each panel shows the same quantity as in Figure 1.

(A color version of this figure is available in the online journal.)

### 3.2. Evolution of Systems Realized with Different Numerical Resolution

In order to investigate the sensitivity of our simulation results to numerical resolution, we compare the orbital evolution of otherwise identical simulations, differing only in numerical resolution from our non-self-gravitating prototype model. One simulation uses half the number of particles used in our prototype ( $\sim 225,000$ ) and a second uses twice that number ( $\sim 900,000$ ). Figure 4 shows the evolution of the planet's orbital elements for all three simulations. The evolution of the orbital elements is nearly identical in all three simulations, until  $\sim 900$  have passed. Given this outcome, we believe that the evolution of the orbital elements seen in our simulations is well resolved.

At late times, the planet's inward migration accelerates in all three simulations, but much more so in the low- and high-resolution variants than at standard resolution. We believe the

difference is due to a slightly more permissive condition placed upon the smoothing length in the low- and high-resolution simulations, than was placed on the standard resolution variation. Specifically, a larger minimum value of the smoothing length for particles was employed for the standard resolution run than the other two. As the planet reenters the disk and began accreting mass from it, smaller smoothing lengths permit comparatively more massive envelopes to develop, resulting in larger perturbations to the dynamical evolution in the low- and high-resolution simulations. We will discuss the significance of the envelope in our simulations in Section 3.5.

### 3.3. Evolution of Systems with Varying Initial Orbital Parameters

Figure 5 shows the migration of the planet for three different initial semimajor axes. In each case, the initial migration phase is characterized by similar inward drift rates which do not significantly depend on the initial location of the planet and also do not significantly depend on the osculating eccentricity and inclination. After the orbits are damped to sufficiently low-inclination—about  $10^\circ$  in each case—migration rates increase because the planets spend more time embedded in the disk where density is high. As noted above for the two 4 AU models, the planets also begin to accumulate an envelope of disk material at this time.

Both eccentricity and inclination are damped rapidly as the disk and the planet interact, with rates that depend slightly on the initial semimajor axis of the planet (Figure 6). The damping is similar to that observed by Cresswell et al. (2007) for high eccentric orbits. In the first phase, the decay is described approximately by  $\dot{e} \propto e^{-2}$  while it becomes exponential when  $e$  is smaller than 0.1, as predicted by the linear analysis of Tanaka & Ward (2004). This last kind of evolution is really observed only for the case with  $a_0 \sim 2$  AU, since the inclination damping is faster in the other two cases ( $a_0 \sim 4$  and 6 AU) and the planet re-embeds itself entirely inside the disk before the eccentricity becomes lower than 0.1. Performing a least-squares fit to the data with a function like that given in Cresswell et al. (2007),

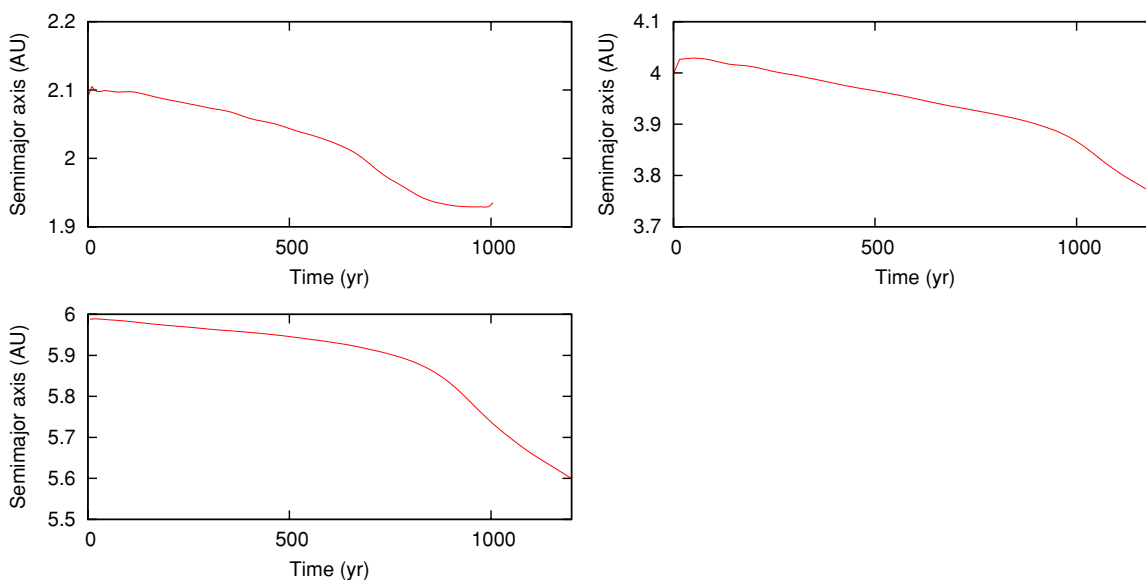


**Figure 5.** Semimajor axis evolution of the planet as a function of time for three different initial semimajor axes, near 2, 4, and 6 AU. Apparent sharp, short term variations in the semimajor axes are artifacts due to our calculation of its instantaneous value based on the planet's position and velocity parameters at the time of each dump.

(A color version of this figure is available in the online journal.)

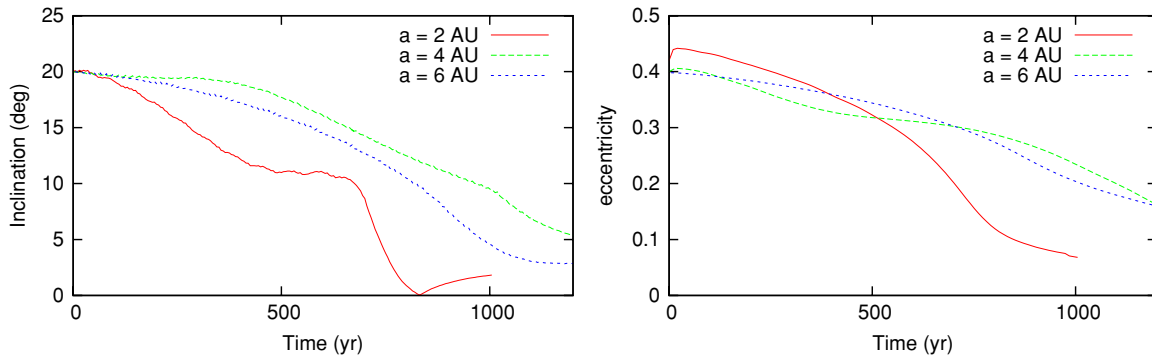


**Figure 6.** Evolution of a planet's eccentricity and inclination. Both the orbital elements are damped by the interactions of the planet with the disk. (A color version of this figure is available in the online journal.)

we find that the damping time down to  $e = 0.1$  is 265 orbital periods,  $T_0$  for  $a_0 \sim 2$  AU,  $154 T_0$  for  $a_0 \sim 4$  AU, and  $103 T_0$  for  $a_0 \sim 6$  AU. This is faster than that found by Cresswell et al. (2007) for a protoplanet with a mass of  $20 M_\oplus$  which is about  $400 T_0$  for  $e_0 = 0.3$ ,  $i_0 = 8^\circ$ , and for  $a_0 \sim 5.2$  AU. A more massive planet evolves more rapidly because its interaction with the disk is stronger.

The inclination damping rates are more sensitive to the initial location in the disk, with the 2 AU model decaying most rapidly. Interestingly, after it begins to accumulate an envelope, the damping increases dramatically. Ultimately the planet passes entirely through the disk, such that its apapsis lies below the disk plane rather than above it, visible in the plot near  $\sim 700$  yr as an inflection point in the value of the inclination. As it reaches low inclination, however, the eccentricity decay slows because essentially all disk matter within reach of the planet's orbit has fallen into its envelope. Little mass remains to provide continuing damping through continuing gravitational torques. Neither of the other two simulations were evolved far enough in time to determine whether they too would produce such behavior. The damping time of the inclination appears to be slightly shorter than that of the eccentricity. As for the eccentricity, a scaling proportional to  $i^2$  can be used to model the initial non-linear damping of inclination. We find that the timescale for damping down to  $6^\circ$  ( $\sim 0.1$  radian) with a least-squared fit is  $212 T_0$  at 2 AU (the fit is poor in this case),  $122 T_0$  at 4 AU and  $64 T_0$  at 6 AU.

If we start the planet with a lower initial eccentricity both the migration rate and the inclination damping are faster. As it can be seen in Figure 7, the planet started with an eccentricity of 0.4 has a slower evolution compared to the cases with  $e_0 = 0.2$  and  $e_0 = 0.0$ . Only after the planet has developed an envelope and has returned to the disk, the orbital behavior is almost independent from the eccentricity. The slower evolution with higher eccentricity is possibly related to the larger vertical distance from the disk at apohelion. A planet on a highly inclined and eccentric orbit spends more time far from the disk compared to one on a circular orbit leading to a lower planet-disk interaction. The effect is not linear with eccentricity since the orbital evolution for both  $e_0 = 0.2$  and  $e_0 = 0.0$  is quite similar, while it is significantly different when the eccentricity grows to  $e_0 = 0.4$ .

Based on the results of these simulations, we conclude that planets excited onto moderately inclined and eccentric orbits will return to a state in which they are embedded within the disk within a few thousand years of the event which originally caused their orbit excitation.

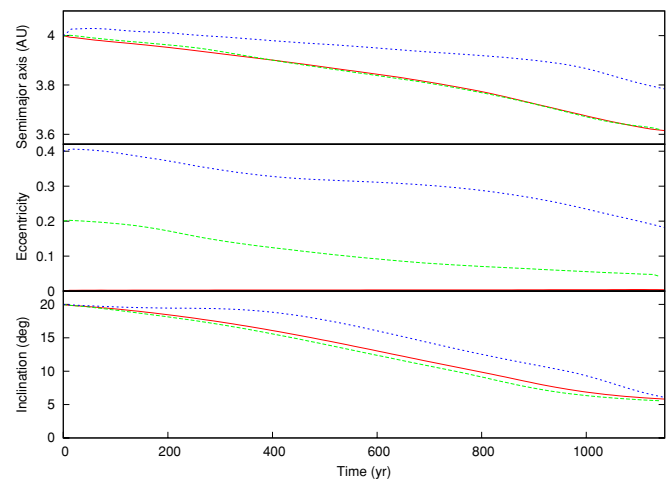


**Figure 7.** Orbital evolution of a planet for three different initial values of eccentricity. Both the migration rate and the inclination damping are faster for lower eccentricities. The red line is for  $e_0 = 0.0$ , the green line for  $e_0 = 0.2$ , and the blue line for  $e_0 = 0.4$ .

(A color version of this figure is available in the online journal.)

#### 3.4. Evolution of Systems Where the Planet has been Scattered into a Disk Cavity

As discussed in the Introduction, a phase of planet-planet scattering may be a consequence of convergent migration of planets. Hydrodynamic simulations of two close planets embedded in the disk (Snellgrove et al. 2001; Papaloizou 2003; Kley et al. 2004, 2005; Nelson & Benz 2003a, 2003b) have shown that they may be able not only to clear of disk material the region in between them but also that inside the orbit of the inner planet forming a cavity. A similar result is also obtained when three planets are considered (Matsumura et al. 2009). When the planets are driven close enough by the outer disk viscous evolution they may undergo either resonance trapping or mutual scattering depending on the physical conditions of the disk. For example, Adams et al. (2008) have shown that ongoing convergence of orbits leads to scattering when the disk is turbulent. A possible outcome of the planet-planet scattering phase in this scenario is that one planet is injected on an inner eccentric and inclined orbit within the cavity while the other(s) is thrown on outer orbits. A similar evolution for a system of two planets has been studied by Moeckel et al. (2008).

Here, we concentrate on a scenario in which a planet is injected into a cavity of the disk, possibly created prior to the scattering phase, where it evolves under the action of the residual

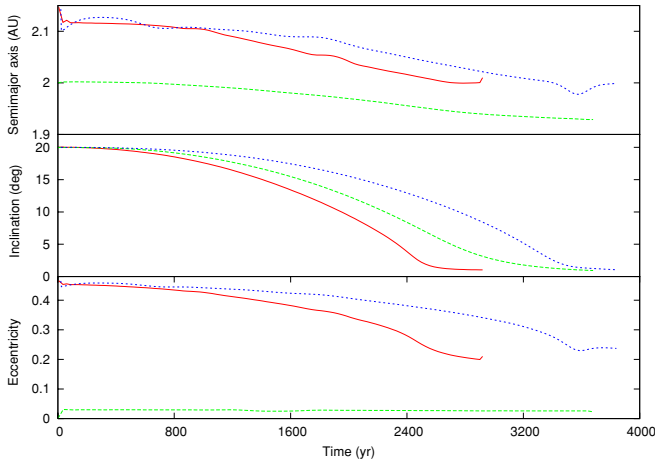


**Figure 8.** Orbital evolution of a planet scattered into a disk cavity on a high-inclination orbit ( $i_p = 20^\circ$ ). The red solid line illustrates the case where the initial eccentricity of the planet is 0.4 and the disk is truncated inside 4 AU. The blue dashed line corresponds to a truncation radius of 5 AU. The green dashed line shows the evolution of a planet on an initially circular orbit embedded in a disk truncated at 4 AU.

(A color version of this figure is available in the online journal.)

outer disk. We start the planet on an orbit with a semimajor axis of 2 AU, an inclination of  $20^\circ$ , and eccentricities of  $e = 0.0$  and  $e = 0.4$ . The disk parameters and the resolution of the numerical model are the same as in the previous simulations, but in this case we truncate the disk inside a given radius. We consider two different models, one where the disk is truncated at 4 AU and one at 5 AU.

In Figure 8, we show the evolution of the orbital elements of the planet. The inclination damping occurs similarly to the case without truncation (Figure 6), but the timescale is longer. The planet returns to the disk plane after about 2500 yr if the truncation radius is at 4 AU, and 3500 yr with the truncation at 5 AU. The inclination damping rate depends on the mass of the disk which is affected by its gravity and the rate is reduced when the disk is less massive. When the truncation is set to 4 AU, the mass of the disk is about  $4.6 M_J$  and it is reduced to  $3.98 M_J$  when the truncation radius is 5 AU. Even the orbital circularization occurs on a longer timescale and the planet has still an eccentricity of about 0.2 when it falls back onto the disk.

The rates and overall magnitudes of semimajor axis migration are consistently smaller compared to the case without truncation (Figure 5). The rates increase with time however, and we postulate that they are related to the increasingly strong interactions with disk material that slowly refills the cavity as the evolution proceeds. The evolution of the disk density profile, averaged over the azimuthal angle, is illustrated in Figure 9 at different evolutionary times for the case with an initial truncation radius of 4 AU. As time passes, gas flows past the truncation radius and resupplies the inner region of the disk, due to both hydrodynamic forces with the disk itself and gravitational perturbations from the still inclined planet.

The cavity is replenished with gas coming from the outer disk only, while the planet remains on an inclined orbit. As soon as the planet reaches the disk, it reopens a gap and evolves as predicted by type II migration. Similar behaviors are observed in both our simulations with a broader initial cavity and those with the planet on an initially circular orbit. The presence of a cavity or of a smaller gap, possibly originating in the planet/disk interactions prior to the planet–planet scattering phase, does not

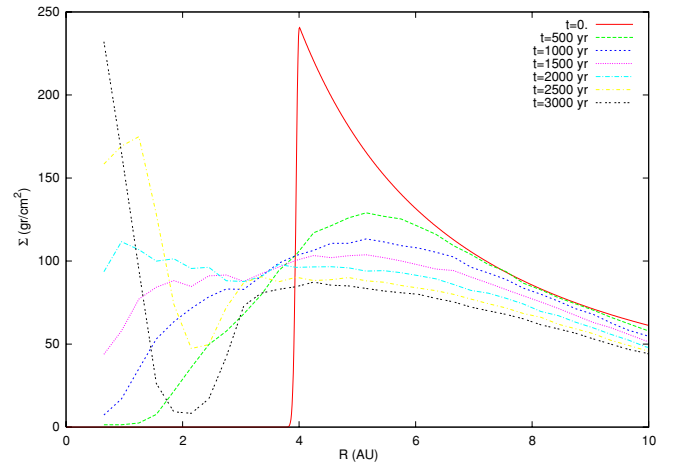


**Figure 9.** Density profile of the disk as a function of the radial distance from the star at different evolutionary times. The gas refills the inner region of the disk until the planet dives back into the disk and opens a gap.

(A color version of this figure is available in the online journal.)

affect significantly the way in which the inclination is damped, but may lead to an increase of the timescale of the damping process. Even if some gas survives in the cavity, as suggested by Crida & Morbidelli (2007) and Lubow & D’Angelo (2006), this would not alter the kind of planet evolution we have described. Again, only the timescale and possibly the eccentricity with which the planet falls back into the disk may be different.

### 3.5. Effects of Accretion and the Planet’s Atmosphere

As a consequence of its presence in the disk, mass accretes onto a forming planet and an envelope grows around it. During times when it spends most of its orbit at high altitude above or below the disk midplane, less mass will accumulate, since that part of its orbit is spent in regions where densities are low. To what extent will accretion continue, while still inclined? Can it be enhanced by repeated encounters with the high-density disk midplane or does efficient accretion require the core to be permanently embedded?

From a theoretical standpoint, it is unclear whether a planet in a highly inclined orbit should have a substantial envelope, accumulated before its orbit was perturbed out of the midplane, or how massive that envelope should be if present. If the high orbital inclination is a consequence of a planet–planet scattering phase, the strong gravitational interactions during the close encounters might have stripped the original atmosphere away. On the other hand, scenarios where high inclination is pumped up by a resonance would appear to be much more complex. In this case, the planet would be gently pushed out of plane over time and might retain its atmosphere.

Our models do not consider accretion of gas (e.g., via absorbing SPH particles directly onto the planet), nor do they include either sufficient resolution or a sufficiently detailed physical model for us to accurately model the formation of an envelope around the planet itself. Therefore, at times when accretion is significant, our results will become less representative of the actual physical behavior than when accretion is not important. With care, however, we shall be able to draw a number of interesting conclusions from our results during both time frames.

Figure 10 shows the mass of material contained in an envelope of one Hill radius,  $R_H$ , in diameter, for each of our three simulations without disk self-gravity. Near the beginning

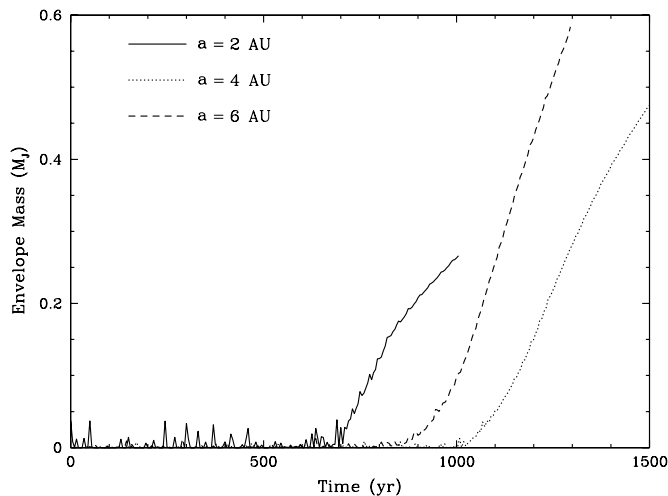


**Figure 10.** Mass accumulation within a volume of one Hill radius in diameter for our simulations with varying initial semimajor axis.

of each simulation, disk material appears inside the Hill volume only when the planet passes through the disk itself, and does not accumulate. Mass begins to accumulate only after the orbit inclinations have decreased to  $\sim 10^\circ$ , approximately 700 yr, 1000 yr, and 900 yr after the simulations themselves begin for the 2 AU, 4 AU, and 6 AU runs, respectively. Once it does, the envelope masses increase monotonically to several tenths of the planet's mass within a few hundred years of additional evolution.

In principle, the presence of an extended envelope is appropriate. It corresponds to the situation in which the envelope is near hydrostatic equilibrium and the gravitational contraction timescale (the Kelvin–Helmholtz time) is longer than the evolutionary timescale under consideration, in this case inclination and eccentricity damping. This will occur when the envelope continues to accrete while the central core of the planet continues to radiate strongly (Pollack et al. 1996; Nelson et al. 2000). As a consequence, any accumulated atmosphere does not fall onto the planet because it is sustained by its own thermal energy.

In fact, however, once accumulation begins, the rates derived from our plots are extremely high, and so are instead more likely due to the breakdown of the assumption that the gas is well modeled by a locally isothermal equation of state. In the neighborhood of the planet, this assumption fails because the gas undergoes substantial compression and because it interacts dynamically with streams of material that enter the Hill volume on different trajectories. Both processes generate thermal energy very quickly, thereby increasing the fluid pressure and throttling further accretion. Additionally, a planet on a significantly inclined orbit will spend most of its time out of the disk, thereby permitting it to be heated further by stellar irradiation. Using an isothermal gas is equivalent to assuming that all of this energy is instantly radiated away so that the pressure remains low and throttling is short circuited, but violating the constraints of Kelvin–Helmholtz contraction noted above.

The fact that essentially no material accumulates in the envelope while its orbit remains inclined, even though our assumptions strongly favor it, supports the physical conclusion that no further accretion occurs during that time. For planets whose inclinations never decay below a threshold of  $\sim 10^\circ$ , this statement is equivalent to the conclusion that they have reached their final masses, perhaps long before the disk itself has decayed away and even while other planets in the system

continue to grow. During this time period we believe that our simulations most accurately reflect the actual evolution of the orbital elements, because accretion plays no role.

Once accumulation begins, the large envelope masses perturb the migration rates, such that after the envelope has formed they are likely to be overestimated. There are at least two reasons of numerical origin to support this conclusion. First, the slight differences in the orbital velocities of the disk material composing the envelope and the planet cause the envelope to exert a large effective drag force, slowing the planet in its orbit and increasing its migration. A similar phenomenon appears in the grid-based simulations of Nelson & Benz (2003a) when the gravitational softening parameter was set smaller than approximately half of one zone, and we believe that the origin of both behaviors is the same.

Second, a numerical phenomenon similar in effect to friction may play an important role in the evolution. As the envelope grows in size, so too does its cross section for interacting with disk material. This is important because the artificial viscosity used in SPH, required for numerical stability, produces far more dissipation in disk simulations due to shear than is appropriate disk simulations, a fact well known to its practitioners. With a large cross section, the planet/envelope combination suffers much greater dissipation than is necessary for flow stability, thereby increasing the migration rates as orbital kinetic energy dissipates in the form of heat. While we employ several techniques to reduce the magnitude of the dissipation (see, e.g., Wetzstein et al. 2009), it is not possible to eliminate it entirely, so the migration will therefore be more rapid than would otherwise occur.

Due to these effects, we expect a slower migration rate and a slower damping of eccentricity and inclination than actually occurs late in our simulations, though still more rapid than the initial evolution when the planet resides primarily outside the disk. Although we cannot rely on the rates for changes in the orbital elements to be fully accurate at late times, we are still able to draw important conclusions from them because they are upper limits. First, we can conclude that the migration of a planet on an inclined orbit will accelerate once its inclination decreases to a value below  $\sim 10^\circ$ , where it again becomes embedded in the disk. Its eccentricity and inclination will also be damped more quickly than occurs at higher inclinations. Systems in which planet–planet scattering has occurred will therefore be observed in configurations where the planets either remain in very different inclinations than the original disk, or in essentially coplanar configurations because the inclinations have been near totally damped.

#### 4. DISCUSSION

When a Jovian planet is ejected out of its protoplanetary disk after a phase of planet–planet scattering or because of resonant interactions, it is rapidly pulled back into the disk. The gravitational interaction between the disk and the planet causes a quick dumping of both the eccentricity and inclination of the planet orbit while, at the same time, the disk becomes warped. The timescale by which the planet returns to the disk midplane is of the order of a few thousand years, significantly faster than that previously found for small planets ( $M \leq 20 M_\oplus$ ). The interaction with the gaseous disk also causes the planet to migrate inward at a rate faster than the viscous one and comparable to that of a terrestrial planet under type I migration. Many different resonances may contribute to this out-of-plane inward orbital migration, including vertical resonances. The



inclination damping is a robust result and also occurs when the planet is injected into a disk cavity, where it interacts with the outer residual disk after a presumed scattering event. The damping rates depend on the amount of gas outside the cavity and on details of how the gas refills the cavity after the planet has been moved to its highly inclined orbit. Our results imply that systems with multiple planets each with different inclination, should have undergone planet–planet scattering after the disk was already dissipated or that a different mechanism acted to stir the inclinations. We can make a similar conclusion for systems in which planetary orbits are misaligned with the stellar spin axis, assuming that the present day stellar spin axis defines the disk plane during formation.

During its evolution far from the disk midplane the planet accretes mass at a very low rate. However, when its inclination is lower than  $\sim 10^\circ$  its accretion rate increases rapidly as mass becomes trapped within its Hill’s sphere. This leads to a faster damping of eccentricity and inclination and also to a more rapid inward migration. Our SPH simulations do not model this last phase accurately because the isothermal approximation fails when gas is accreted and compressed in proximity of the planet and it also interacts with streams of material entering the Hill’s sphere on different trajectories.

The problem of the interaction of the disk with the growing atmosphere of the planet is a very complex, beyond the aim of this paper. One simple method to improve our numerical modeling in the last stages of the planet evolution when it starts to accrete disk mass could be to adopt an ‘ad hoc’ accretion rate of the material within the Hill’s sphere, as implemented in numerous previous works. Unfortunately, the details of the accretion prescription do not provide much physical insight, as they must be chosen rather arbitrarily.

The scenario we outline with our model generates many questions in need of further investigation. For example, during planet–planet scattering in presence of the gas in the protostellar disk, how much of the planet envelope is lost during mutual close encounters? Is the tidal force strong enough to strip each planet of a significant amount of gas? What is the thermodynamical state of the envelope after a sequence of close encounters?

As the planet returns to the disk, how quickly does the envelope reform? Does it reform quickly into a hydrostatic configuration? How massive? Does it trigger a revisit of the core instability phase during which the planet originally gained most of its mass? Does infalling disk material instead produce a highly dynamically active envelope, as was seen for lower mass cores in Nelson & Ruffert (2005)?

An additional interesting aspect is to understand what happens when an additional giant planet is added to the system, either on an inclined or planar orbit. Is the interaction between the disk and the inclined planet different? Do the out-of-plane perturbations of one planet affect the gap formation of the non-inclined planet?

If both are on inclined orbits, is the damping less efficient leading to longer timescales? What happens when one planet is inside a disk cavity and the other just outside of it?

We thank an anonymous referee for his useful comments and suggestions. Parts of this work were carried out under the auspices of the National Nuclear Security Administration of the U.S. Department of Energy at Los Alamos National Laboratory under Contract No. DE-AC52-06NA25396, for which this is publication number LA-UR 09-03432.

## REFERENCES

- Adams, F. C., Laughlin, G., & Bloch, A. M. 2008, *ApJ*, **683**, 1117
- Alibert, Y., Mordasini, C., Benz, W., & Winisdoerffer, C. 2005, *A&A*, **434**, 343
- Baruteau, C., & Masset, F. 2008, *ApJ*, **678**, 483
- Chatterjee, S., Ford, E. B., Matsumura, S., & Rasio, F. A. 2008, *ApJ*, **686**, 580
- Cresswell, P., Dirksen, G., Kley, W., & Nelson, R. P. 2007, *A&A*, **473**, 329
- Crida, A., & Morbidelli, A. 2007, *MNRAS*, **377**, 1324
- Durisen, R. H., Boss, A. P., Mayer, L., Nelson, A. F., Quinn, T., & Rice, W. K. M. 2007, in *Protostars and Planets V*, ed. B. Reipurth, D. Jewitt, & K. Keil (Tucson, AZ: Univ. of Arizona Press), 607
- Griv, E. 2007, *ApJ*, **665**, 866
- Kley, W., Lee, M. H., Murray, N., & Peale, S. J. 2005, *A&A*, **437**, 727
- Kley, W., Peitz, J., & Bryden, G. A. 2004, *A&A*, **414**, 735
- Larwood, L. D., Nelson, R. P., Papaloizou, J. C. B., & Terquem, C. 1996, *MNRAS*, **282**, 597
- Lubow, S. H., & D’Angelo, G. 2006, *ApJ*, **641**, 526
- Lubow, S. H., & Ogilvie, G. I. 2001, *ApJ*, **560**, 997
- Marzari, F., & Weidenschilling, S. J. 2002, *Icarus*, **156**, 570
- Matsumura, S., Thommes, E. W., Chatterjee, S., & Rasio, F. A. 2009, arXiv:0903.2660v1
- Moeckel, N., Raymond, S. N., & Armitage, P. J. 2008, *ApJ*, **688**, 1361
- Moorhead, A. V., & Adams, F. C. 2005, *Icarus*, **178**, 517
- Murray, C. D., & Dermott, S. F. 1999, *Solar System Dynamics* (Cambridge: Cambridge Univ. Press)
- Nelson, A. F. 2006, *MNRAS*, **373**, 1039
- Nelson, A. F., & Benz, W. 2003a, *ApJ*, **589**, 556
- Nelson, A. F., & Benz, W. 2003b, *ApJ*, **589**, 578
- Nelson, A. F., Benz, W., & Ruzmaikina, T. V. 2000, *ApJ*, **529**, 357
- Nelson, R. P., Papaloizou, J. C. B., Masset, F., & Kley, W. 2000, *MNRAS*, **318**, 18
- Nelson, A. F., & Ruffert, M. 2005, in *ASP Conf. Ser. 341, Chondrites and the Protoplanetary Disk*, ed. A. N. Krot, E. R. D. Scott, & B. Reipurth (San Francisco, CA: ASP), 903
- Nelson, A. F., Wetzstein, M., & Naab, T. 2009, *ApJS*, **184**, 326
- Papaloizou, J. C. B. 2003, *Celest. Mech. Dyn. Astron.*, **87**, 53
- Papaloizou, J. C. B., & Larwood, J. D. 2000, *MNRAS*, **315**, 823
- Pollack, J. B., Hubickyj, O., Bodenheimer, P., Lissauer, J. J., Podolak, M., & Greenzweig, Y. 1996, *Icarus*, **124**, 62
- Rasio, F. A., & Ford, E. B. 1996, *Science*, **274**, 254
- Snellgrove, M. D., Papaloizou, J. C. B., & Nelson, R. P. 2001, *A&A*, **374**, 1092
- Tanaka, H., Takeuchi, T., & Ward, W. 2002, *ApJ*, **565**, 1257
- Tanaka, H., & Ward, W. 2004, *ApJ*, **602**, 388
- Thommes, E. W., & Lissauer, J. J. 2003, *ApJ*, **597**, 566
- Ward, W. R. 1997, *Icarus*, **126**, 261
- Weidenschilling, S. J., & Marzari, F. 1996, *Nature*, **384**, 619
- Wetzstein, M., Nelson, A. F., Naab, T., & Burkert, A. 2009, *ApJS*, **184**, 298